

# Anisotropic Fusion-product Generation and Emission Spectra in Beam-injected DT Plasmas

Hideaki MATSUURA and Yasuyuki NAKAO

*Department of Applied Quantum Physics and Nuclear Engineering,  
Kyushu University, Motoooka 744, Fukuoka 819-0395, Japan*

(Received: 25 October 2009 / Accepted: 26 January 2010)

The double differential emission spectra for fusion-produced alpha-particle and neutron as a function of emission energy and angle relative to the direction of beam injection are examined on the basis of the one dimensional (1D) Boltzmann-Fokker-Planck (BFP) model in beam-injected (non-Maxwellian) deuterium-tritium (DT) plasmas. It is shown that owing to the existence of energetic component in fuel-ion energy distribution functions due to mono-directional neutral-beam injection (NBI) and/or nuclear elastic scattering (NES), the angular distributions of the emission spectra have highly anisotropic and broadened configuration compared with Gaussian distribution. The shape of the spectra and the fraction of the energetic ( $>3.5$  MeV alpha-particle and  $>14.1$  MeV neutron) components to the total generation rate are quantitatively evaluated for various plasma conditions.

**Keywords:** neutral beam injection heating, knock-on tail formation, alpha-particle emission spectrum, nuclear elastic scattering, Boltzmann-Fokker-Planck equation

## 1. Introduction

Energetic ions in a burning plasma have important roles in various stages of fusion-reactor operations. The non-Maxwellian tail is created by neutral-beam-injection (NBI) and/or ion cyclotron range of frequencies (ICRF) heating. The knock-on tail is also formed due to nuclear elastic scattering (NES) of fast ions[1-4]. The non-thermal fusion has been examined[5,6] for a number of decades and suitable models to predict the non-thermal fusion yields have been developed[7]. In conceptual designs of next-generation fusion devices, however, use of deuterium beam-injection energy much higher than the current experiments, e.g. 1 MeV, is considered[8]. In such a case, the effects of NES on fractional beam-energy deposition to ions[9,10] and  $T(d,n)^4\text{He}$  reaction rate coefficient[11] can be appreciable. The effect on the modification of the fusion-product emission spectrum can also be appreciable. We have investigated the modification of alpha-particle emission spectrum assuming isotropic beam injection[12] (ion velocity distribution functions,  $\alpha$ -particle and neutron emission spectra have been treated in one-dimensional velocity space assuming uniform plasmas). In the actual case, however, external beam is injected in a specific direction, so the emission spectra of  $\alpha$ -particle and neutron would have anisotropic distributions. In such a case, asymmetric  $\alpha$ -particle generation with energy above 3.5 MeV may influence the plasma confinement and sustainment properties. The detailed estimation for the alpha-particle behaviors in burning plasma would be important.

For the purpose of analyzing the alpha-particle

behavior in the burning plasmas, it would be required to accurately grasp the characteristics of fusion-produced alpha-particle source. In this paper, the 2-dimensional (2D) fusion source, i.e. alpha-particle double differential emission spectrum, as well as neutron double differential spectrum as a function of energy and emitting direction (the angle between the direction of alpha-particle (neutron) emission and that of beam injection) are quantitatively evaluated for various plasma parameters.

We consider a DT plasma accompanied with injection of a mono-energetic and mono-directional deuterium beam. To facilitate the analysis, on the basis of the 1-D Boltzmann-Fokker-Planck (BFP) model [10-11,13], the velocity distribution functions of deuterium and tritium are first derived simultaneously considering the broadened alpha-particle emission spectrum in the energy space. Using the obtained deuterium and tritium distribution functions, we examine the  $T(d,n)^4\text{He}$  fusion reaction between the mono-directional deuterium distribution and isotropic background tritium distribution function. The double differential emission spectra of alpha-particle and neutron due to  $T(d,n)^4\text{He}$  fusion reaction are evaluated as a function of birth energy and emission angle relative to the beam-injection direction. It is shown that the modification of the spectra is influenced by the tail formation in both deuterium and tritium distribution functions due to beam injection and NES, and the fractions of energetic ( $> 3.52$  MeV) alpha-particle and energetic ( $> 15$  MeV) neutron significantly increase or decrease due to the modification of the emission spectra depending on the emission directions.

---

author's e-mail: mat@nucl.kyushu-u.ac.jp

## 2. Analysis Model

### 2.1 Boltzmann-Fokker-Planck model

The BFP equation for ion species  $a$  ( $a = D, T$  and  $\alpha$ -particle) is written as

$$\sum_j \left( \frac{\partial f_a}{\partial t} \right)^C + \sum_i \left( \frac{\partial f_a}{\partial t} \right)_i^{\text{NES}} + \frac{1}{v^2} \frac{\partial}{\partial v} \left( \frac{v^3 f_a}{2\tau_c^*(v)} \right) + S_a(v) - L_a(v) = 0, \quad (1)$$

where  $f_a(v)$  is the velocity distribution function of the species  $a$ . The first term in the left-hand side of Eq.(1) represents the effect of the Coulomb collision[14]. The summation is taken over all background species, i.e.  $j = D, T$ , alpha-particle and electron. The collision term is hence non-linear, retaining collisions between ions of the same species. The second term accounts for the NES of species  $a$  by background ions[10-11,13]. We consider NES between 1)  $\alpha$ -particle and D, and 2)  $\alpha$  and T, i.e.  $(a,i) = (D,\alpha), (T,\alpha), (\alpha,D)$  and  $(\alpha,T)$ . The NES cross-sections are taken from the work of Perkins and Cullen[2].

The third term in the left-hand side of Eq.(1) represents the diffusion in velocity space due to thermal conduction. To incorporate the unknown loss mechanism of energetic ion into the analysis, following Bittoni's treatment[15], we simulate the velocity dependence of the energy loss due to thermal conduction  $\tau_c^*(v)$  and the particle-loss time  $\tau_p^*(v)$  by using a dimensionless parameter  $\gamma$ , i.e.

$$\tau_{c(p)}^*(v) = \begin{cases} C_{c(p)} \tau_{c(p)} & \text{when } v < v_{th} \\ C_{c(p)} \tau_{c(p)} (v/v_{th})^\gamma & \text{when } v \geq v_{th} \end{cases}, \quad (2)$$

The high exponent  $\gamma$  chosen ensures rapid increment of both confinement times in higher energy range compared with the one in the thermal energy range, and thus energetic particle itself and its energy are hardly evacuated compared with that of thermal particle. In this paper throughout the calculations  $\gamma = 4$  is assumed. As was discussed in Ref.10, in usual plasma condition, the  $\gamma$  would not be a significant parameter as far as we choose sufficiently large values, e.g.  $\gamma \geq 4$ . Considering energy loss mechanisms both due to thermal conduction and particles transport loss from plasma, the global energy confinement time is defined as  $1/\tau_E = 1/\tau_C + 1/\tau_P$ . (see Ref.10-11,13).

The source ( $S_a(v)$ ) and loss ( $L_a(v)$ ) terms take different form for every ion species. For deuteron, the source and loss terms are described so that the fueling, beam-injection, transport loss and the loss due to T(d,n)<sup>4</sup>He reaction are balancing each other[10-11];

$$S_D(v) - L_D(v) = \frac{S_D}{4\pi v^2} \delta(v - v_D^{\text{fueling}})$$

$$+ \frac{S_{NBI}}{4\pi v^2} \delta(v - v_D^{NBI}) - \zeta_D f_D - \frac{f_D(v)}{\tau_p^*(v)}. \quad (3)$$

Here  $v_D^{\text{fueling}}$  indicates the speed of the fueled deuteron, which is much smaller than the thermal speed, i.e. nearly equal to zero. The fueling rate  $S_D$  is determined so that the deuteron density is kept constant, i.e.

$$S_D = \frac{n_D}{\tau_p} + n_D n_T \langle \sigma v \rangle_{DT} - S_{NBI}. \quad (4)$$

The  $S_{NBI}$  is the NBI rate per unit volume and  $v_D^{NBI}$  is the speed corresponding to injected beam energy  $E_{NBI}$ . We express the injection rate  $S_{NBI}$  using the beam energy  $E_{NBI}$  and injection power  $P_{NBI}$ , i.e.  $S_{NBI} = P_{NBI} / (E_{NBI} V)$ . Here  $V$  represents the plasma volume. Referring to the design parameter for ITER[8], we assume  $V = 800 \text{ m}^3$ .

The T(d,n)<sup>4</sup>He reaction rate coefficient is written as

$$\langle \sigma v \rangle_{DT} = \frac{4\pi}{n_D n_T} \int v_D^2 \zeta_D(v_D) \times f_D(v_D) dv_D, \quad (5)$$

with

$$\zeta_D = \frac{2\pi}{v_D} \int v_T f_T(v_T) \times \left[ \int_{|v_D - v_T|}^{v_D + v_T} dv_r v_r^2 \sigma_{DT}(v_r) \right] dv_T. \quad (6)$$

The T(d,n)<sup>4</sup>He fusion cross has been taken from the work of Bosch[16].

For triton the NBI injection term is not included in Eq.(3), and the source and loss terms are described so that the fueling rate, transport loss and the loss due to T(d,n)<sup>4</sup>He reaction are balancing [10-11,13].

For alpha-particle, the source and loss terms are written as

$$S_\alpha(v) - L_\alpha(v) = S_\alpha(v) - \frac{f_\alpha(v)}{\tau_p^*(v)}, \quad (7)$$

where NBI and fueling rate in Eq.(3) are replaced by the alpha-particle generation rate due to T(d,n)<sup>4</sup>He reaction,

$$S_\alpha(v) = \frac{(dE/dv)}{4\pi v^2} \int \frac{d^2 N_\alpha}{dE d\Omega_{lab}} d\Omega_{lab}, \quad (8)$$

where  $N_\alpha(E)$  represents the alpha-particle generation rate, which is described in the next section, and  $\Omega_{lab}$  is a unit vector in the direction of emission of the particle in the laboratory system.

## 2.2 alpha-particle and neutron emission spectra

The double differential alpha-particle (neutron) emission energy spectrum is written as

$$\frac{d^2 N_{\alpha(n)}}{dE d\Omega_{lab}}(E, \theta_{lab}) = \iiint f_D(\vec{v}_D) f_T(\vec{v}_T) \frac{d\sigma}{d\Omega} \times \delta(E - E_{\alpha(n)}) \delta(\Omega_{lab} - \Omega_{\alpha(n)}) v_r d\vec{v}_D d\vec{v}_T d\Omega, \quad (9)$$

where  $E_{\alpha(n)}$  is the  $\alpha$ -particle (neutron) energy in the laboratory system[17];

$$E_{\alpha(n)} = \frac{1}{2} m_{\alpha(n)} V_c^2 + \frac{m_{n(\alpha)}}{m_\alpha + m_n} (Q + E_r) + V_c \cos \theta_c \sqrt{\frac{2m_n m_\alpha}{m_n + m_\alpha} (Q + E_r)}, \quad (10)$$

where  $m_{\alpha(n)}$  is the  $\alpha$ -particle (neutron) mass,  $V_c$  is the centre-of-mass velocity of the colliding particles,  $\theta_c$  is the angle between the centre-of-mass velocity and the  $\alpha$ -particle (neutron) velocity in the centre-of-mass frame,  $Q$  is the reaction  $Q$ -value, and  $E_r$  represents the relative energy given by

$$E_r = \frac{1}{2} \frac{m_D m_T}{m_D + m_T} |\vec{v}_D - \vec{v}_T|^2. \quad (11)$$

The  $\theta_{lab}$  represents the angle between the direction of emitted  $\alpha$ -particle (neutron) and that of beam injection in the laboratory system, and  $\Omega_{\alpha(n)}$  is a unit vector in the direction of emission of the alpha-particle (neutron) in the laboratory system, which is determined using the classical kinematics as a function of  $\vec{v}_D$ ,  $\vec{v}_T$  and  $\theta_c$ . From the alpha-particle emission spectrum, the source term of BFP equation for alpha-particle, i.e. Eq.(8), is determined. By means of the computational iterative method, the energy spectrum and the deuteron, triton and alpha-particle velocity distribution functions are consistently obtained. Throughout the calculations the differential  $T(d,n)^4\text{He}$  cross section is assumed to be isotropic in the centre-of-mass frame. As was described previously, in this paper, although the energy distribution of the deuteron distribution function is taken into account, the beam-deuteron is assumed to have mono-directional distribution. The background triton has been assumed to be isotropic distribution as derived by solving Eq.(1).

## 3. Results and Discussion

In Fig.1 we first show the deuteron distribution functions as a function of deuteron energy when 10, 40 and 100 MW NBI heating are made. In the calculations, electron temperature  $T_e = 20\text{keV}$ , the ion densities  $n_D = n_T = 3 \times 10^{19} \text{m}^{-3}$ , energy and particle confinement

times  $\tau_E = (1/2)\tau_p = 3\text{sec}$  and beam-injection energy  $E_{NBI} = 1\text{MeV}$  are assumed. The electron density has different values according to the NBI heating power as  $6.6 - 7.0 \times 10^{19} \text{m}^{-3}$ . The dotted line in deuteron distribution function denotes Maxwellian distribution at 20 keV temperature. The bold line represents the distribution function when no NBI heating is made. We can see that the non-Maxwellian tail due to NBI is formed in the energy range below 1 MeV in the distribution functions. The relative intensity of the tail is increased by NBI with increasing beam-injection powers. The NES is a non-Coulombic, large-angle scattering process, and a large fraction of the fast-ion energy is transferred in a single

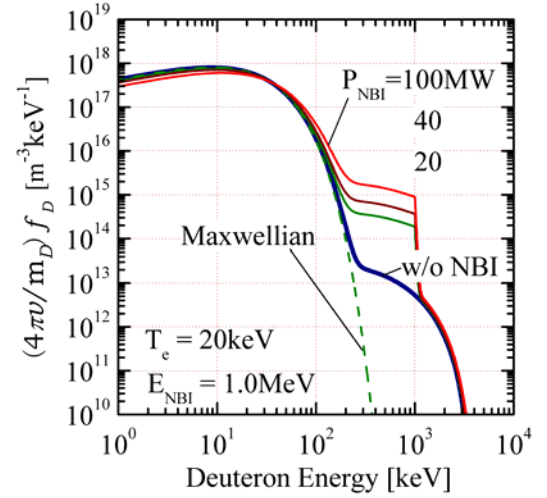


**Fig.1** Deuteron distribution functions when 20, 40 and 100 MW NBI heating are made. The dotted line denotes Maxwellian when no NBI heating is made.

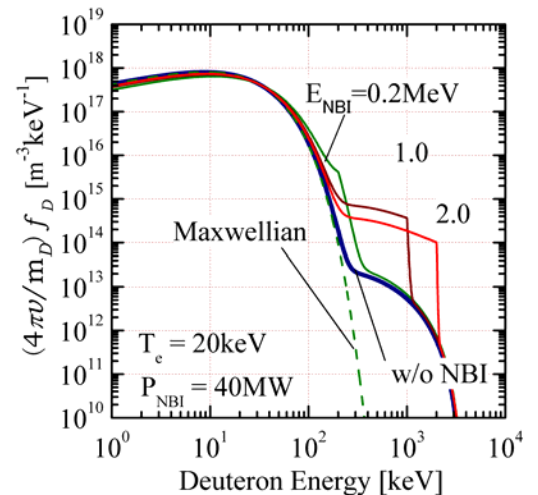


**Fig.2** Deuteron distribution function when NBI heating is made with 0.2, 1.0 and 2.0-MeV beam-injection energies with 40 MW power.

event. Owing to the NES of energetic alpha-particle by low-energy fuel ion, the energetic component, i.e. knock-on tail, is created in the fuel-ion distribution function. The knock-on tail due to NES of alpha-particle is observed in the energy range above 1 MeV in the distribution functions. In Fig.2 the deuteron distribution function are shown for several beam-injection energies. The NBI heating power is taken as 40MW, and other

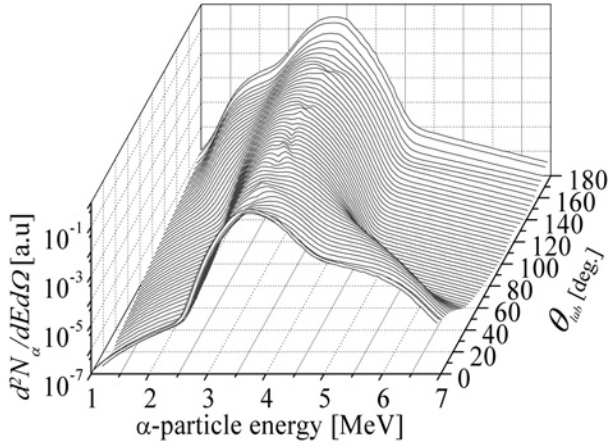


**Fig.3** The double differential emission spectrum for alpha-particle as a function of alpha-particle energy and emission angle relative to the beam-injection direction in the laboratory system.  $P_{NBI}=40\text{MW}$ ,  $E_{NBI}=1.0\text{ MeV}$ ,  $T_e=20\text{ keV}$ ,  $n_e=6.7\times 10^{19}\text{ m}^{-3}$  and  $\tau_E=(1/2)\tau_p=3.0\text{ sec}$  are assumed.

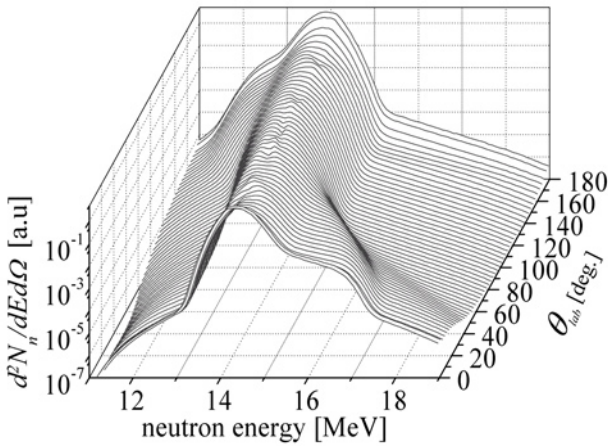


**Fig.4** The double differential emission spectrum for neutron as a function of neutron energy and emission angle relative to the beam-injection direction in the laboratory system.  $P_{NBI}=40\text{ MW}$ ,  $E_{NBI}=1.0\text{ MeV}$ ,  $T_e=20\text{ keV}$ ,  $n_e=6.7\times 10^{19}\text{ m}^{-3}$  and  $\tau_E=(1/2)\tau_p=3.0\text{ sec}$  are assumed.

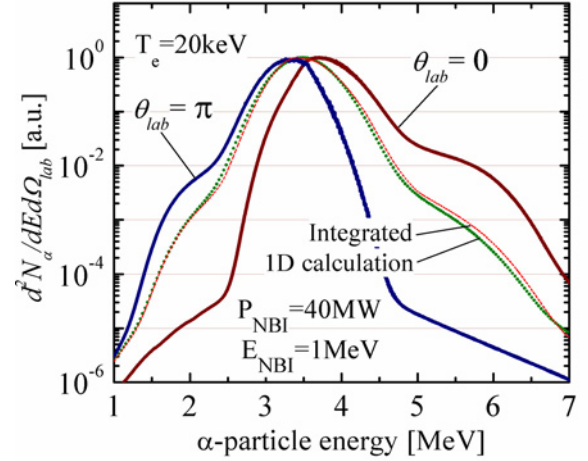


**Fig.5** Comparison between double differential spectrum for alpha-particle (solid lines) and the spectrum derived in 1D calculation (dotted line). The thin line represents the spectrum obtained by integrating the double differential spectrum with respect to  $\theta_{lab}$ .  $P_{NBI}=40\text{ MW}$ ,  $E_{NBI}=1.0\text{ MeV}$ ,  $T_e=20\text{ keV}$  and  $n_e=6.7\times 10^{19}\text{ m}^{-3}$  are assumed.

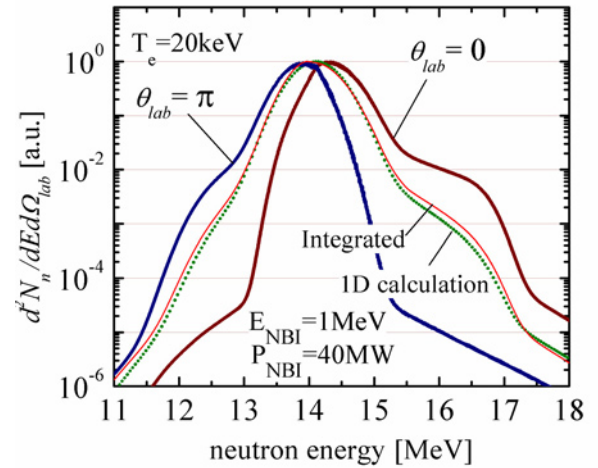


**Fig.6** Comparison between double differential spectrum for neutron (solid lines) and the spectrum derived in 1D calculation (dotted line). The thin line represents the spectrum obtained by integrating the double differential spectrum with respect to  $\theta_{lab}$ .  $P_{NBI}=40\text{ MW}$ ,  $E_{NBI}=1.0\text{ MeV}$ ,  $T_e=20\text{ keV}$  and  $n_e=6.7\times 10^{19}\text{ m}^{-3}$  are assumed.

plasma parameters are the same as those in Fig.1. The electron density has different values as  $6.6-7.0\times 10^{19}\text{ m}^{-3}$  depending on the beam-injection energy  $E_{NBI}$ . It is shown that the fraction of the energetic deuteron increases with increasing beam-injection energy.

In Fig.3 (Fig.4) the normalized double differential spectrum for fusion-born alpha-particle (neutron) is exhibited as a function of alpha-particle (neutron) energy



and emission angle relative to the beam-injection direction in the laboratory system. The NBI power is taken as 40MW, and other calculation parameters are the same as those in Fig.1. It is found that the alpha-particle and neutron emission spectra are broadened toward both low and high energy regions, and fraction of the alpha-particle (neutron) born with more than 3.5 MeV (14 MeV) energy increases compared with the Gaussian distribution function. We can also find that in the beam-injection direction, i.e.  $\theta_{lab} = 0$ , the fraction of the energetic alpha-particle (neutron)

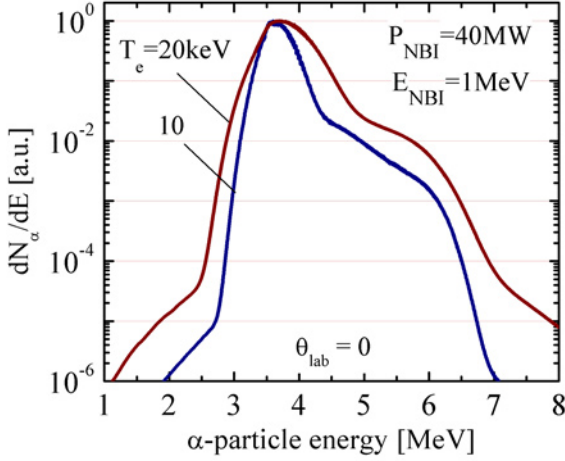


**Fig.7** The alpha-particle emission spectra in the beam-injection direction ( $\theta_{lab}=0$ ) for various electron temperatures as a function of alpha-particle energy in the laboratory system.  $P_{NBI}=40$  MW,  $E_{NBI}=1.0$  MeV are assumed.

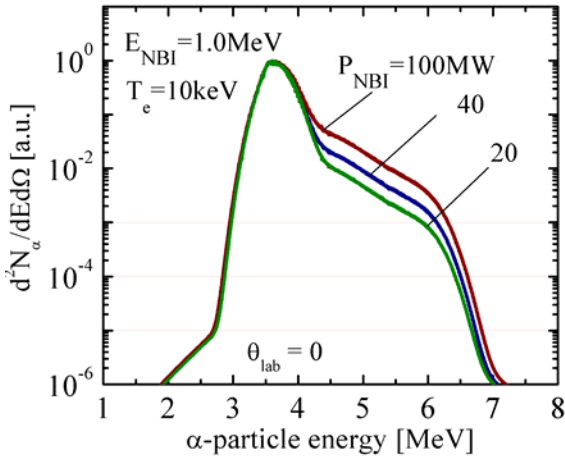


**Fig.8** The alpha-particle emission spectra in the beam-injection direction ( $\theta_{lab}=0$ ) for several  $P_{NBI}$  as a function of alpha-particle energy in the laboratory system.  $T_e=10$  keV,  $E_{NBI}=1.0$  MeV are assumed.

component significantly increases. On the contrary in the opposite direction relative to injected beam direction, i.e.  $\theta_{lab} = \pi$ , the fraction of the energetic alpha-particle (neutron) significantly decreases. Since injected beam energy is much higher than the mean energy of the bulk-ion component, the center-of-mass velocity has almost the same value as the injected-beam velocity. The alpha-particle (neutron) is produced almost isotropic direction in the center-of-mass frame, and hence the alpha-particle (neutron) which is emitted toward beam-injection direction, i.e.  $\theta_{lab} = 0$ , has considerably higher energy compared with the one which is emitted toward the opposite direction, i.e.  $\theta_{lab} = \pi$ , in the laboratory system.

In Fig.5 (Fig.6) the energy spectra of alpha-particle (neutron) in the  $\theta_{lab} = 0$  and  $\pi$  directions are shown as well as the spectrum derived in the 1D calculation. The calculation condition is the same as those in Fig.3 and 4. We can see the spectrum has highly anisotropic distributions depending on the emission angle. The thin line represents the spectrum obtained by integrating the double differential spectrum with respect to  $\theta_{lab}$ . It seems that the shape of the integrated spectrum is almost close to the one derived in the 1D calculation. To quantitatively estimate the distortion of the spectrum, the following parameter is introduced;

$$F_{>E_{cut}}(\theta_{lab}) = \frac{\int_{E_{cut}}^{\infty} \left( \frac{d^2 N_j}{dE d\Omega_{lab}} \right) dE}{\int_0^{\infty} \left( \frac{d^2 N_j}{dE d\Omega_{lab}} \right) dE}, \quad (12)$$

which implies the fraction of the alpha-particle (neutron) generation with the energy above  $E_{cut}$  to total generation in the specific ( $\theta_{lab}$ ) direction. For example, the cut-off energy  $E_{cut}$  can be chosen as  $E_{cut} = 4$  MeV (15 MeV) for alpha-particle (neutron). The fractions when the modification is considered  $F_{>E_{cut}}$  and when Gauss distribution is assumed  $F_{>E_{cut}}^{Gauss}$  are evaluated, and the increment in the fraction due to the modification, i.e.  $F_{>E_{cut}}/F_{>E_{cut}}^{Gauss}$ , is estimated. When electron temperature  $T_e = 20(10)$  keV, electron density  $n_e = 6.7(6.2) \times 10^{19} \text{ m}^{-3}$ , NBI power  $P_{NBI} = 40$  MW and energy  $E_{NBI} = 1$  MeV (see Fig.5), if we only look at the alpha-particles which is emitted in  $\theta_{lab} = 0$  direction, the fraction of the alpha-particle generation with energy above 4 MeV to total  $\theta_{lab} = 0$  alpha-particle component reaches 25.1 (10.1)%, which is roughly 3.3 (5.6) times larger than the value when Gaussian distribution is assumed, i.e. 7.7 (1.8) %. If we look at the  $\theta_{lab} = \pi$  direction, the fraction of the alpha-particle generation with energy above 4 MeV to total  $\theta_{lab} = \pi$  alpha-particle component is 0.64 (0.11)%, which is roughly 1/12 (1/17) times larger than the value when Gaussian distribution is assumed. For neutron in the same plasma condition (see Fig.6), the fraction of the

neutron generation with energy above 15 MeV to total  $\theta_{lab} = 0$  neutron component reaches 3.3 (2.3)%, which is roughly 13.0 (1100.0) times larger than the value when Gaussian distribution is assumed for the neutron emission spectrum, i.e. 0.26 (0.0021) %.

In Fig.7 the  $\theta_{lab} = 0$  component of the alpha-particle double differential spectrum is shown for two cases of electron temperature, i.e.  $T_e = 10$  keV and 20 keV. The other parameters are same as those in Fig.5. In low temperature range, the Gaussian distribution has narrow half width, and hence broadness of the spectrum becomes relatively small. In the same manner, the dependence of the spectrum on  $P_{NBI}$  is also examined and presented in Fig.8. We can see the energetic, i.e.  $> 4$  MeV, component increases with increasing  $P_{NBI}$  as was previously denoted in Fig.1.

In this paper the double differential emission spectra for alpha-particle and neutron produced by  $T(d,n)^4He$  reaction have been investigated. Throughout the calculations, the following assumptions have been made: (a) deuteron has mono-directional distribution function, (b) background triton has isotropic distribution function and (c) the differential  $T(d,n)^4He$  cross section is isotropic in the center-of-mass system. In actual plasmas accompanied with NBI heating, the deuteron distribution function has 2D configuration and triton distribution may be also anisotropic distribution function. In such a case, if we could reflect the exact 2D velocity distribution function in the calculation, the  $F_{>E_{cut}}$  value might be somewhat smaller compared with the present calculations. In  $E_{NBI} < 1$  MeV range, the anisotropy of the differential  $T(d,n)^4He$  cross section in the center-of-mass frame would not be significant so much. An anisotropic suprathermal component in the fuel-ion distribution would also be created by ICRF heating. By improving the present model so that we can include the 2D distribution function effect, the double differential emission spectra for fusion products in ICRF-heated plasma can also be estimated.

If the alpha-particle emission spectrum has an anisotropic distribution, the alpha-particle velocity distribution function itself may also have an anisotropic configuration. The transport processes, e.g. first-orbit loss, of alpha-particle in the fusion devices would be affected by the particle energy. The fractional energy deposition from alpha-particle to bulk ions and electrons via collisions is also changed depending on the relative velocity between alpha and bulk particles. The modification of the alpha-particle emission spectrum, e.g. increment in the number of energetic ( $\geq 3.5$  MeV) alpha-particle, may influence the alpha-heating characteristics. We performed considerably rough estimation for the effect of alpha-particle spectrum modification on the transit alpha-particle loss, and obtained the result that when electron temperature  $T_e = 20$  keV, the electron density  $n_e = 4.2 \times 10^{19} \text{ m}^{-3}$ ,

energy and particle confinement times  $\tau_E = (1/2)\tau_p = 3 \text{ sec}$ , beam-injection energy  $E_{NBI} = 1$  MeV and power  $P_{NBI} = 40 \text{ MW}$  are assumed, the alpha-particle loss increased several percent compared with the case when mono-energetic (3.5 MeV) alpha-particle source is assumed[18]. In the estimation, isotropic alpha-particle generation was assumed. If we could consider the anisotropic alpha-particle emission spectrum derived in this paper, the influence on the confinement would be further enhanced depending on the direction of the beam-injection. Further detailed studies for modification of the double differential emission spectra, and as a next step issue, investigation of the effect of the spectrum modification on the alpha-particle behaviors in burning plasma would be required for various plasma conditions.

#### 4. References

- [1] J. J. Devany and M. L. Stein, Nucl. Sci. Eng. **46**, 323 (1971).
- [2] S. T. Perkins and D. E. Cullen, Nucl. Sci. Eng., **20**, 77 (1981).
- [3] L. Ballabio, G. Gorini, J. Källne, Phys. Rev. E, **55**, 3358 (1997).
- [4] J. Källne, L. Ballabio, J. Frenje, S. Conroy, G. Ericsson, M. Tardocchi, E. Traneus, et al., Phys. Rev. Lett, **85**, 1246 (2000).
- [5] R. J. Hawryluk, Rev. Mod. Phys. **70**, 537 (1998).
- [6] JET Team (prepared by P.R. Thomas), Nucl. Fusion **39**, 1619 (1999).
- [7] R. V. Budny, M. G. Bell, A. C. Janos, M. G. Bell, A. C. Janos, D. L. Jassby, L. C. Johnson, D. K. Mansfield, D. C. McCune, H. Redi, J. F. Schivell, G. Taylor, T. B. Terpstra, M. C. Zamstorf, S. J. Zweben, Nucl. Fusion **35**, 1497 (1995).
- [8] R. Aymar, Fusion Eng. Des., **55**, 107 (2001).
- [9] H. Matsuura, Y. Nakao, K. Kudo, Nucl. Fusion, **39**, 145 (1999).
- [10] H. Matsuura, Y. Nakao, Phys. Plasmas, **13**, 062507 (2006).
- [11] H. Matsuura, Y. Nakao, Phys. Plasmas, **14**, 054504 (2007).
- [12] H. Matsuura, Y. Nakao, Phys. Plasmas, **16**, 042507 (2009).
- [13] M. Nakamura, Y. Nakao, V. T. Voronchev, K. Hegi, H. Matsuura, O. Mitarai, J. Phys. Soc. Jpn. **75**, 024801 (2006).
- [14] M. N. Rosenbluth, W. M. MacDonald, D. L. Judd, Phys. Rev. **107**, 1 (1957).
- [15] E. Bittoni, J. G. Cordey, M. Cox, Nucl. Fusion **29**, 931 (1980).
- [16] H. -S. Bosch and G. Hale, Nucl. Fusion **32**, 611 (1992).
- [17] G. Lehner and F. Pohl, Z. Phys., **207**, 83 (1967).
- [18] T. Fukue, H. Matsuura, Y. Nakao, to be published in *Proc. APFA/APTTC2009*, Aomori, Japan, 2009.